International Journal of Heat and Technology
Vol. 44, No. 1, February, 2026, pp. 19-33
Journal homepage: http://iieta.org/journals/ijht

Electromagnetic–Thermal Energy Conversion Pathway Analysis and Multiphysics Collaborative Optimization Based on a Generalized Thermodynamic Potential

Ran Zhou[1,2], Keqilao Meng[2,3*], Dajiang Jia[4]

[1] College of Energy and Power Engineering, Inner Mongolia University of Technology, Hohhot 010051, China
[2] Key Laboratory of Wind Energy and Solar Energy, Ministry of Education, Hohhot 010051, China
[3] School of Renewable Energy, Inner Mongolia University of Technology, Ordos 017010, China
[4] Shanghai Ghrepower Green Energy Co., Ltd., Shanghai 201600, China

Corresponding Author Email: mengkeqilao23@163.com

https://doi.org/10.18280/ijht.440103

Received: 11 October 2025
Revised: 9 February 2026
Accepted: 18 February 2026
Available online: 28 February 2026

Keywords:
generalized thermodynamic potential, electromagnetic–thermal coupling, physics-informed deep potential network, entropy production constraint, differentiable topology optimization

ABSTRACT

In electromagnetic–thermal multiphysics coupling optimization, conventional methods often suffer from the lack of thermodynamic consistency, inaccurate prediction of energy conversion pathways, and low optimization efficiency, making them inadequate for meeting the core requirements of complex thermodynamic systems in terms of energy conversion efficiency and thermodynamic performance. To address these challenges, this paper proposes a physics-informed deep potential network (PIDPN)–based collaborative optimization framework for electromagnetic–thermal multiphysics systems. Taking the generalized thermodynamic potential as the central state variable, the framework enables precise analysis of electromagnetic-to-thermal energy conversion pathways and coordinated system topology optimization. The key innovations of the proposed framework are as follows. First, a deep neural network is employed to implicitly represent the generalized thermodynamic potential, while automatic differentiation is used to derive field quantities and key thermodynamic parameters, thereby overcoming the limitations of traditional discrete modeling approaches. Second, a composite loss function incorporating the second law of thermodynamics is constructed, where the non-negativity constraint of entropy production ensures the physical consistency of the predictions. Third, an end-to-end differentiable collaborative optimization architecture is designed to integrate physical field prediction with material topology design, enabling unified simulation and optimization and significantly improving optimization efficiency. The proposed method eliminates the need for mesh discretization and large amounts of labeled data, naturally adapts to complex geometric boundaries, and accurately captures the irreversible conversion mechanisms between electromagnetic and thermal energy, thereby substantially enhancing the thermodynamic performance of the system. The proposed approach can be widely applied to complex thermodynamic systems such as induction heating, thermoelectric energy conversion, and thermal management in nuclear fusion devices. It provides a novel thermodynamics-based modeling and design paradigm for multiphysics collaborative optimization, with significant academic value and promising engineering applications.

1. INTRODUCTION

Electromagnetic–thermal energy conversion is a typical irreversible thermodynamic process in industrial production and energy utilization, and its conversion efficiency and thermodynamic performance directly determine the operating level of complex systems [1, 2]. Multiphysics collaborative optimization [3-5], as a core means to improve energy conversion efficiency and reduce system entropy production, has become a research hotspot in the fields of thermodynamics and energy science. However, traditional electromagnetic–thermal multiphysics analysis and optimization methods have fundamental defects, which severely restrict the design and performance improvement of complex thermodynamic systems and cannot meet the stringent requirements of advanced equipment for thermodynamic accuracy and efficiency. Discrete mesh-based simulation methods [6, 7] rely on mesh discretization, which not only introduces unavoidable numerical discretization errors, but also fails to satisfy the strict mathematical requirements of continuity and differentiability of the generalized thermodynamic potential, leading to systematic deviations in the prediction of electromagnetic–thermal energy conversion pathways. Explicit constitutive relation modeling [8, 9] requires manually predefined coupling response rules of material fields and cannot adaptively capture the nonlinear thermodynamic behavior of materials under complex operating conditions, which further causes prediction results to violate fundamental

thermodynamic principles, commonly resulting in distorted entropy production rate predictions and even physically unreasonable phenomena such as negative entropy production. The separated optimization mode [10, 11] completely separates physical field simulation from topology design. The optimization process requires repeated calls to independent solvers, which is not only inefficient, but also fails to unify field coupling mechanisms and topology design from the thermodynamic essence, causing the optimization results to often fall into local optima and making it difficult to achieve global improvement of system thermodynamic performance. Therefore, constructing theories and methods that can strictly guarantee thermodynamic consistency, accurately capture irreversible conversion laws, and efficiently realize collaborative optimization has become a core bottleneck that urgently needs to be broken through in the current fields of thermodynamics and multiphysics optimization.

Physics-informed neural network (PINN) provides a new technical pathway for multiphysics modeling, but its application in electromagnetic–thermal coupled thermodynamic systems still have limitations that are difficult to overcome and has not solved the core pain points of traditional methods. Existing PINN models mostly take direct fitting of field quantities as the core and do not treat the generalized thermodynamic potential as the core state variable. They lack deep integration with thermodynamic principles and cannot essentially describe the intrinsic laws of irreversible electromagnetic–thermal energy conversion [12, 13]. At the same time, the loss function design of existing models usually only considers the basic constraints of electromagnetic fields and energy conservation, without introducing the rigid constraint of the second law of thermodynamics, which cannot guarantee the thermodynamic consistency of prediction results, resulting in a significant decline in their generalization ability and prediction accuracy under complex operating conditions [14, 15]. In the fields of topology optimization and multiphysics coupling, existing studies are still limited to separated design ideas based on explicit thermodynamic models, relying on artificially constructed constitutive relations and empirical parameters. This not only makes the modeling process cumbersome and poorly adaptable, but also fails to realize the organic collaboration among physical field simulation, thermodynamic constraints, and topology optimization, making it difficult to balance optimization efficiency and optimization quality. More importantly, all current related studies have not broken through the core dilemma that "thermodynamic principles are disconnected from deep modeling and collaborative optimization," and have not constructed an integrated framework with thermodynamic potential as the core that runs through the entire process of modeling and optimization. This research gap directly leads to the fact that electromagnetic–thermal multiphysics optimization cannot get rid of the limitation of "emphasizing simulation while neglecting thermodynamic essence," and thus it is difficult to achieve fundamental improvement of system thermodynamic performance.

In view of the core defects of existing studies and the key research gaps mentioned above, this paper takes the generalized thermodynamic potential as the core state variable, deeply embeds the first and second laws of thermodynamics into the entire process of neural network design and optimization, and constructs a physics-informed deep potential network (PIDPN) collaborative optimization framework to realize precise modeling of electromagnetic–thermal multiphysics fields, precise analysis of conversion pathways, and efficient optimization of system topology, thereby fundamentally solving the core problems of lack of thermodynamic consistency, insufficient prediction accuracy, and low optimization efficiency in existing methods.

The core research content of this paper focuses on technical breakthroughs from the perspective of thermodynamics. First, a deep parameterized representation method of the generalized thermodynamic potential is constructed. Through implicit neural representation, the limitations of traditional discrete modeling are overcome, and precise derivation of field quantities and key thermodynamic parameters is achieved. Second, a composite loss function incorporating the second law of thermodynamics is designed, in which the non-negative constraint of entropy production rate ensures the physical consistency of prediction results and compensates for the lack of rigid thermodynamic constraints in existing models. Third, an end-to-end differentiable collaborative optimization architecture is proposed, connecting physical field prediction with material topology design to achieve the integration of simulation and optimization and completely solve the problem of low efficiency in separated optimization. Finally, through numerical verification of typical electromagnetic–thermal thermodynamic systems, the effectiveness, superiority, and universality of the method are comprehensively validated. The structure of this paper is arranged as follows: Section 2 elaborates the theoretical basis and overall framework design; Sections 3–5 present in detail the technical details of the three core innovations; Section 6 introduces the network architecture and training strategy; Section 7 analyzes the method performance through numerical verification; Section 8 discusses the innovative significance, limitations, and future directions of the research; Section 9 summarizes the conclusions of the paper.

2. THEORETICAL BASIS AND CORE FRAMEWORK

2.1 Core thermodynamic theoretical support

Thermodynamics of irreversible processes is the core theoretical support of the method in this paper. Its core criteria include energy conservation [16, 17] and non-negative entropy production rate [18, 19], which together determine the thermodynamic essence of the irreversible conversion from electromagnetic energy to thermal energy. The expression of the law of energy conservation in an electromagnetic–thermal coupled system is:

$$\rho c_p \frac{\partial T}{\partial t} = \nabla \cdot (k \nabla T) + Q_j + Q_m \tag{1}$$

where, ρ is the material density, c_p is the specific heat capacity at constant pressure, k is the thermal conductivity, Q_j is the Joule heat source, and Q_m is the hysteresis/dielectric loss heat source. This equation explicitly defines the energy transfer and conservation law of electromagnetic energy conversion into thermal energy. The local entropy production rate, as the core representation of irreversible processes, must satisfy the non-negative constraint, and its expression is:

$$\dot{S}_{gen} = \frac{k}{T^2} (\nabla T)^2 + \frac{J \cdot E}{T} \tag{2}$$

where, J is the current density, E is the electric field intensity, and T is the temperature, which respectively reflect the influence of heat conduction irreversibility and electromagnetic dissipation irreversibility on the thermodynamic performance of the system. The generalized thermodynamic potential function $\Psi(x,t;\theta)$, as the core variable describing the thermodynamic state of the system [20, 21], where x is the spatial coordinate, t is time, and θ is the trainable parameters of the network. Its derivative relations can directly derive the electromagnetic field, temperature field, and various thermodynamic parameters, providing a solid thermodynamic theoretical basis for subsequent deep modeling and collaborative optimization.

2.2 Overall design of the physics-informed deep potential network collaborative optimization framework

The PIDPN collaborative optimization framework proposed in this paper takes the generalized thermodynamic potential function as the core bridge, connecting three modules: physical field prediction, thermodynamic constraints, and topology optimization, realizing seamless integration of electromagnetic–thermal energy conversion pathway analysis and system optimization. From the perspective of architecture design, it breaks through the core dilemma of separation between simulation and optimization in traditional methods. The specific architecture is shown in Figure 1. The framework adopts a parallel dual-branch architecture corresponding to the physical field prediction branch and the material topology design branch, respectively. The two branches share spatial coordinate inputs but their parameters are trained independently, ensuring that thermodynamic constraints run through the entire process of modeling and optimization. This architecture differs from the limitation of existing PINN that only focus on physical field simulation with a single branch, and realizes the integration of thermodynamic principles, deep modeling, and collaborative optimization. The physical field prediction branch takes the generalized thermodynamic potential function $\Psi(x,t;\theta)$ as the core output target. A multilayer perceptron combined with sinusoidal activation functions is used to construct the network, directly outputting electric field intensity E, magnetic field intensity H, and temperature T, and then using automatic differentiation technology to derive key thermodynamic parameters such as electromagnetic energy flux density $S = E \times H$, Joule heat source $Q_J = J \cdot E$, and entropy production rate $\dot{S}_{gen}$. The material topology design branch outputs the spatial distributions of material electrical conductivity $\sigma(x)$ and thermal conductivity $k(x)$ through a material distribution parameterization network $\phi(x;\xi)$, where ξ represents the trainable parameters of the material network. The collaborative linkage between the two branches realizes the integration of physical field simulation and topology optimization without repeatedly calling independent solvers, ensuring that the optimization process always follows basic thermodynamic principles such as energy conservation and non-negative entropy production rate. This provides an architectural guarantee for precise analysis of electromagnetic–thermal energy conversion pathways and improvement of system thermodynamic performance.

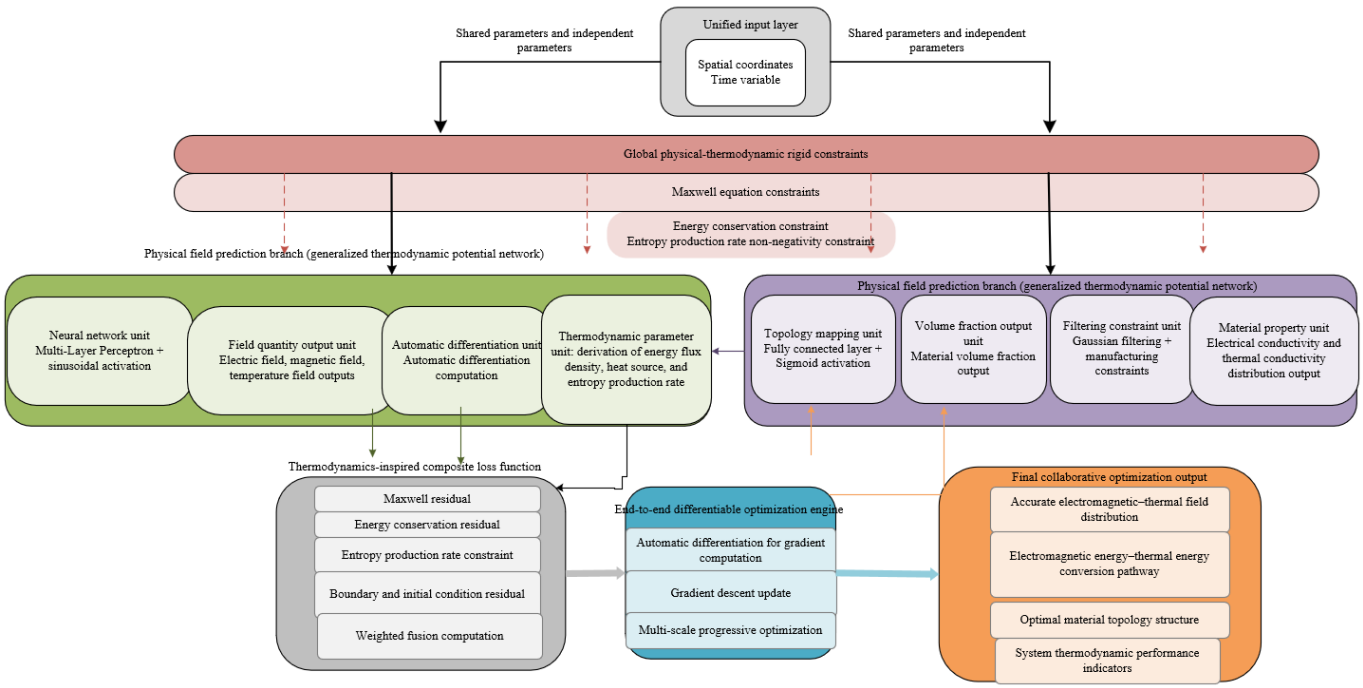

Figure 1. Schematic diagram of the overall architecture of the physics-informed deep potential network (PIDPN) collaborative optimization framework

3. DEEP PARAMETERIZED REPRESENTATION OF THE GENERALIZED THERMODYNAMIC POTENTIAL

This paper, for the first time, takes the generalized thermodynamic potential function $\Psi(x,t;\theta)$ as the core output variable of the neural network, breaking through the inherent limitation of directly fitting field quantities in traditional multiphysics modeling, realizing the deep integration of thermodynamic principles and deep learning, and constructing a deep parameterized representation method of the generalized thermodynamic potential that combines physical consistency

and representation accuracy. This representation method adopts a multilayer perceptron combined with sinusoidal activation functions to construct the network architecture. The spatial coordinate vector $x=(x_1,x_2,x_3)$ and time t are taken as the network inputs, and the electric field intensity vector $E(x,t)$, magnetic field intensity vector $H(x,t)$, and temperature scalar $T(x,t)$ are directly output as three key physical quantities. The network output relationship can be expressed as:

$$[E(x,t),H(x,t),T(x,t)]=\Psi(x,t;\theta) \tag{3}$$

where, θ is the set of trainable parameters of the network, including the weights and biases of each layer. Based on automatic differentiation technology, by taking derivatives of the generalized thermodynamic potential function Ψ, all core thermodynamic and electromagnetic parameters can be reversely derived without manually deriving the coupling relationships among field quantities. The electromagnetic energy flux density is obtained by the cross product of electric field intensity E and magnetic field intensity H, $S = E \times H$. Combined with the current density $J = \sigma E$, where σ is the material electrical conductivity, the Joule heat source can be obtained by dot product, $Q_j = J \cdot E = \sigma E \cdot E$. Based on thermodynamics of irreversible processes, the local entropy production rate can be further derived from the temperature gradient and electric field intensity:

$$\dot{s}_{gen}=\frac{k}{T^2}(\nabla T)^2+\frac{\sigma E\cdot E}{T} \tag{4}$$

In this way, the thermodynamic coherence of the electromagnetic–thermal energy conversion process and the accuracy of parameter derivation are ensured from the source of modeling, fundamentally changing the situation in which thermodynamic principles are disconnected from deep learning in traditional modeling. Figure 2 shows the principle diagram of implicit parameterized representation of the generalized thermodynamic potential and field quantity derivation.

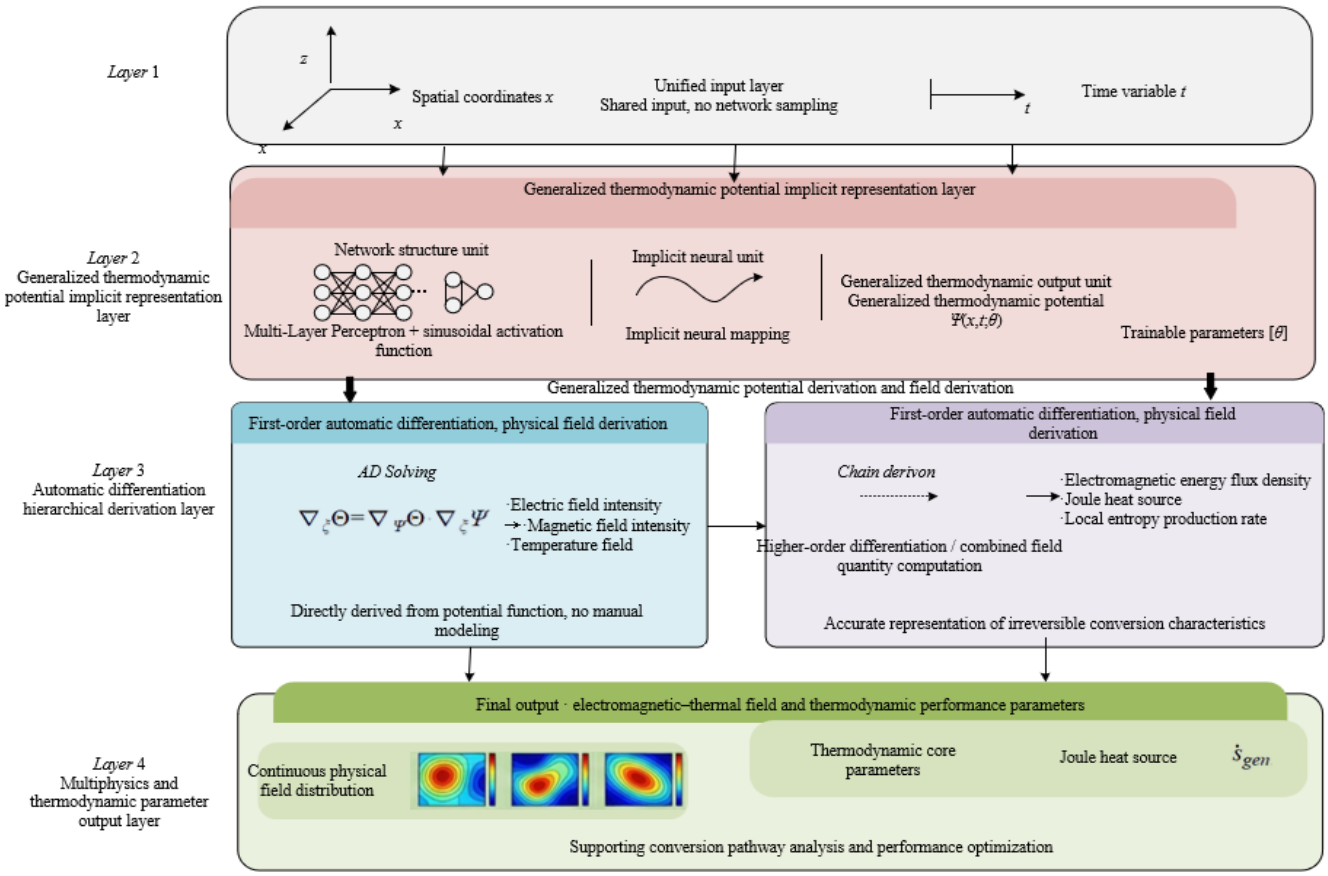

Figure 2. Principle diagram of implicit parameterized representation of the generalized thermodynamic potential and field quantity derivation

The deep parameterized representation of the generalized thermodynamic potential adopts an implicit neural representation method, which shows significant technical advantages from the thermodynamic perspective, perfectly matching the strict mathematical requirements of the generalized thermodynamic potential for state variables, and the technical details can be implemented and verified. Mesh-free design is one of the core advantages of this representation method. It does not require mesh discretization of the solution domain, and directly realizes the continuous representation of the generalized thermodynamic potential function in the entire solution domain through the implicit mapping of the neural network, effectively avoiding the numerical discretization error brought by traditional discrete mesh methods and ensuring that $\Psi(x, t; \theta)$ satisfies the thermodynamic requirement of spatial continuity of state variables, thus providing the basis for precise analysis of electromagnetic–thermal energy conversion pathways. The infinitely differentiable property is realized through automatic differentiation technology. The network output function $\Psi(x,$

t; θ) can efficiently complete the calculation of derivatives of any order, that is, $\nabla\Psi$, $\partial\Psi/\partial t$, $\nabla^2\Psi$, etc. can all be directly obtained through network backpropagation, perfectly matching the core requirements of the generalized thermodynamic potential for continuity and differentiability, and effectively solving the problem that traditional explicit modeling methods cannot simultaneously consider macro–mesoscopic scale coupling and cannot accurately capture the details of irreversible conversion. At the same time, this representation method does not require complex mesh discretization and boundary discrete processing, and can naturally couple arbitrary complex geometric boundaries. Through the adaptive learning of spatial coordinates by the network, it can directly adapt to different types of electromagnetic–thermal thermodynamic systems, breaking through the limitation that traditional discrete modeling methods are restricted by geometric shapes and complicated boundary processing, and greatly improving the universality of the representation method. Figure 3 shows the schematic comparison between mesh-free implicit representation and traditional mesh discrete modeling.

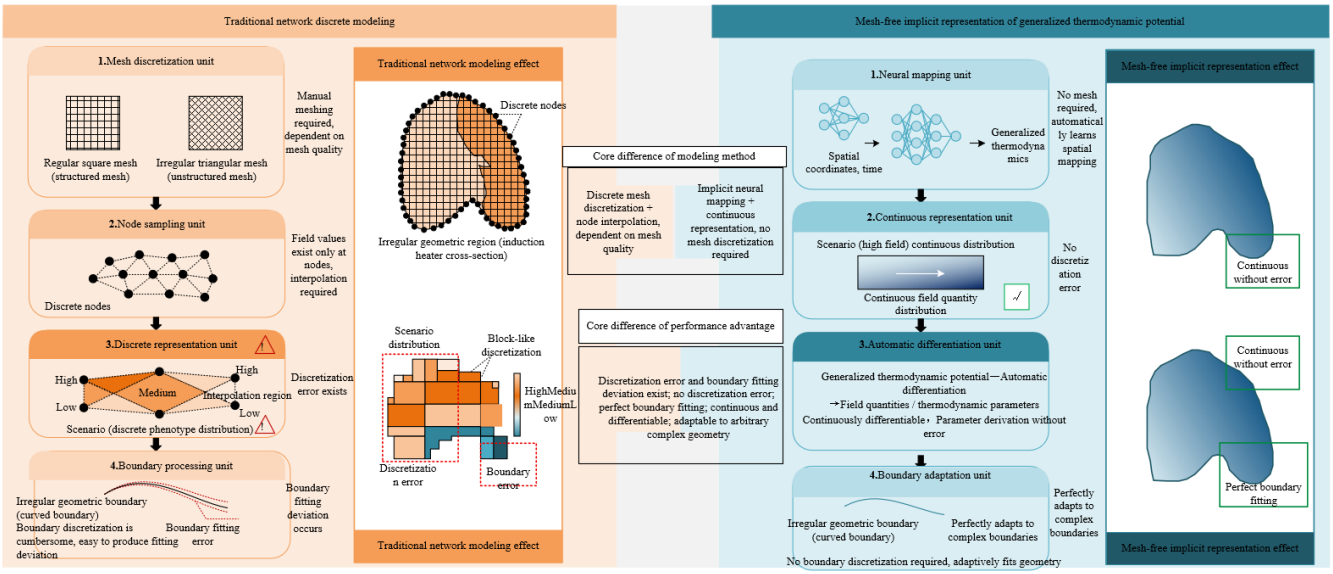

Figure 3. Schematic comparison between mesh-free implicit representation and traditional mesh discrete modeling

4. THERMODYNAMICS-INSPIRED MULTIPHYSICS COUPLED LOSS FUNCTION

The multiphysics coupled loss function constructed in this paper takes thermodynamic laws as the core rigid constraints and follows the design principle of unsupervised training. It aims to solve the core problems of poor generalization and lack of physical consistency in traditional data-driven methods, and to achieve accurate modeling of the network without relying on large amounts of labeled data. Its core design logic is to deeply embed the first and second laws of thermodynamics and the fundamental laws of electromagnetic fields into the loss function. By minimizing the residuals of each physical constraint, the network output is forced to strictly follow the physical essence, ensuring the thermodynamic rationality of the electromagnetic energy–thermal energy conversion pathway. The overall loss function adopts a weighted summation form, taking into account the importance of each constraint and training stability. The total loss function is expressed as:

$$L_{total}=\alpha L_{maxwell}+\beta L_{energy}+\gamma L_{entropy}+\delta L_{bc} \tag{5}$$

where, α, β, γ, and δ are the adaptive weight coefficients of each residual term, which can be dynamically adjusted according to the satisfaction degree of each constraint during training, ensuring the convergence of the training process and the effective satisfaction of each physical law, and realizing the deep binding of thermodynamic principles and network training from the source of design.

Each component of the loss function has a clear division of responsibilities and works collaboratively, which not only ensures the strict satisfaction of electromagnetic field and thermodynamic laws, but also takes into account training stability and generalization. The technical details can be implemented and verified. The Maxwell equation residual term is used as an auxiliary constraint. Through automatic differentiation technology, the curl and divergence of the electric field intensity and magnetic field intensity are calculated, forcing the network output to satisfy the fundamental laws of electromagnetic fields. Its residual expression is:

$$L_{maxwell}=\|\nabla\times E+\frac{\partial B}{\partial t}\|_2^2+\|\nabla\times H-J\|_2^2 \tag{6}$$

where, B is the magnetic flux density, which provides the basis for electromagnetic–thermal coupled modeling and avoids the prediction of field quantities violating the essence of electromagnetics. The generalized energy conservation residual term is the core embodiment of the first law of thermodynamics. It unifies electromagnetic energy and thermal energy into the energy conservation framework. The hysteresis/dielectric loss heat source is derived from the partial derivatives of the generalized thermodynamic potential function Ψ with respect to the electromagnetic fields:

$$Q_m=\frac{\partial\Psi}{\partial E}\cdot E+\frac{\partial\Psi}{\partial H}\cdot H \tag{7}$$

Combined with the Joule heat source $Q_j = \sigma E\cdot E$, the

complete energy conservation equation is constructed:

$$\rho c_p \frac{\partial T}{\partial t} - \nabla \cdot (k \nabla T) - Q_j - Q_m = 0 \tag{8}$$

The residual expression is:

$$L_{energy} = \left\| \rho c_p \frac{\partial T}{\partial t} - \nabla \cdot (k \nabla T) - Q_j - Q_m \right\|^2 \tag{9}$$

In this way, the thermodynamic unified representation of electromagnetic energy–thermal energy conversion can be realized, which is different from the limitation of traditional modeling where energy conservation and electromagnetic losses are modeled separately. The entropy production rate constraint term, as the rigid constraint of the second law of thermodynamics, is the core innovation of the loss function. Based on thermodynamics of irreversible processes, the local entropy production rate $\dot{s}_{gen}$ must satisfy the non-negative constraint. Therefore, it is constructed as a penalty term:

$$L_{entropy} = \left\| \max(0, -\dot{s}_{gen}) \right\|_2^2 \tag{10}$$

The constraint strength is adjusted through the adaptive penalty coefficient γ, ensuring that the field distribution predicted by the network strictly satisfies the requirement of non-negative entropy production rate, thus solving the key problem that existing methods ignore thermodynamic consistency and lead to distorted entropy production rate prediction. The boundary and initial condition residual terms adopt a combination of soft constraints and hard constraints. Hard constraints are used for key boundaries, and the boundary conditions are directly embedded into the input–output mapping of the network. Soft constraints are used for non-key boundaries, and the constraints are realized through residual terms:

$$L_{bc} = \|E - E_{bc}\|_2^2 + \|H - H_{bc}\|_2^2 + \|T - T_{bc}\|_2^2 \tag{11}$$

where, E_{bc}, H_{bc}, and T_{bc} are the reference values of electric field, magnetic field, and temperature at the boundary, respectively. In this way, the satisfaction of boundary conditions is ensured while avoiding the decline of network generalization caused by excessive constraints, and adapting to the boundary requirements of different thermodynamic systems.

5. END-TO-END DIFFERENTIABLE ELECTROMAGNETIC–THERMAL COLLABORATIVE OPTIMIZATION ARCHITECTURE

This paper proposes an end-to-end differentiable electromagnetic–thermal collaborative optimization architecture, which breaks through the inherent limitations of traditional separated optimization and realizes the integration of physical field simulation, sensitivity analysis, and topology optimization. The core lies in the deep connection between the material distribution parameterization network and the physical field prediction network, and the construction of a differentiable optimization chain based on automatic differentiation technology, ensuring that the optimization process always follows the basic principles of thermodynamics. A material distribution parameterization network $\phi(x;\xi)$ is introduced. The network structure is constructed using fully connected layers combined with a Sigmoid activation function. The spatial coordinate x is taken as input, and the material volume fraction $\phi(x)$ is output. Through the mapping relationship, it is transformed into the spatial distributions of electrical conductivity $\sigma(x) = \sigma_{max}\phi(x) + \sigma_{min}(1-\phi(x))$ and thermal conductivity $k(x) = k_{max}\phi(x) + k_{min}(1-\phi(x))$, where σ_{max} and σ_{min} are the maximum and minimum electrical conductivity of the material, respectively, k_{max} and k_{min} are the maximum and minimum thermal conductivity of the material, respectively, and ξ is the trainable parameter of the material network. The material network ϕ and the physical field prediction network Ψ are connected in series. The physical field network completes the prediction of electromagnetic–thermal fields and thermodynamic parameters based on $\sigma(x)$ and $k(x)$ output by the material network. The optimization objective is defined as the thermodynamic quality factor $\Theta = \int_\Omega \dot{s}_{gen}\, dV$, that is, minimizing the total entropy production rate of the system. Through automatic differentiation technology, the gradient of Θ with respect to the material network parameter ξ is directly calculated as $\nabla_\xi \Theta = \nabla_\Psi \Theta \cdot \nabla_\xi \Psi$. The parameter ξ is adaptively updated using the gradient descent method to realize the dynamic optimization of material distribution, which completely solves the core problem of repeatedly calling independent solvers and low efficiency in traditional optimization. Figure 4 shows the schematic diagram of the end-to-end differentiable electromagnetic–thermal collaborative optimization chain.

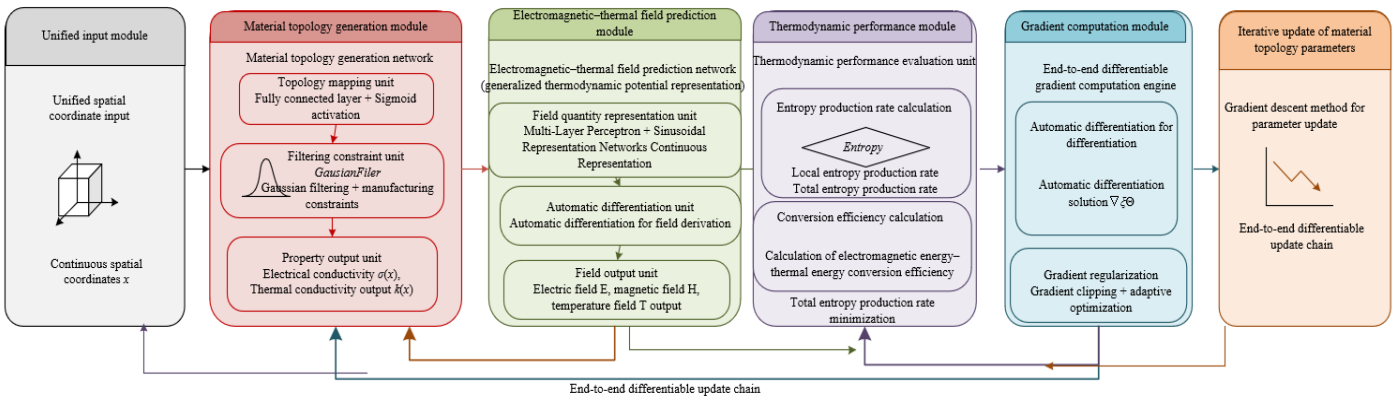

Figure 4. Schematic diagram of the end-to-end differentiable electromagnetic–thermal collaborative optimization chain

To improve the optimization convergence speed, avoid local optima, and enhance engineering practicality, this paper proposes a multi-scale progressive optimization strategy for the first time, combined with the embedding design of manufacturing constraints, to achieve the collaborative improvement of optimization efficiency, topology accuracy, and engineering feasibility. The strategy is promoted in two stages. In the first stage, a low-capacity network is used to train the material network and the physical field network, quickly converging to the initial material topology, focusing on ensuring the correctness of the optimization direction and reducing the computational cost of the initial optimization. In the second stage, the capacities of the two networks are gradually increased by increasing the number of neurons and deepening the number of network layers to refine the material topology structure and improve the topology accuracy. At the same time, the smooth convergence of the optimization process is ensured to avoid training oscillations caused by sudden changes in network capacity. To solve the "checkerboard" problem commonly occurring in traditional topology optimization, a Gaussian filtering layer is introduced after the output layer of the material network. The material volume fraction is smoothed through the filtering function:

$$\phi_{filtered}(x)=\frac{1}{V_\Omega}\int_\Omega \phi(x')G(x-x')dV' \tag{12}$$

where, G is the Gaussian kernel function and V_Ω is the volume of the filtering window, ensuring that the optimized material topology has clear boundaries and a preset minimum feature size. At the same time, the filtering process does not destroy the coupling relationship between material properties and physical fields, ensuring that the thermodynamic constraints such as energy conservation and non-negative entropy production rate are always satisfied during the topology update process, greatly improving the engineering practicality of the method.

The optimization objective of this architecture strictly follows the thermodynamics-oriented research direction, taking the minimization of the thermodynamic quality factor as the core and focusing on the improvement of the thermodynamic efficiency of electromagnetic energy–thermal energy conversion. This is different from the traditional optimization objectives that focus on mechanical performance and electromagnetic performance, highlighting the innovative value from the thermodynamic perspective. The optimization objective Θ can be flexibly defined according to actual needs, mainly including two types of thermodynamic indicators. The first is the total entropy production rate of the system:

$$\Theta_1=\int_\Omega \dot{s}_{gen}\,dV=\int_\Omega\left(\frac{k}{T^2}(\nabla T)^2+\frac{\sigma E\cdot E}{T}\right)dV \tag{13}$$

Its minimization can effectively reduce the irreversible loss in the process of electromagnetic energy–thermal energy conversion and improve the thermodynamic efficiency of energy conversion. The second is the temperature uniformity index:

$$\Theta_2=\frac{1}{V_\Omega}\int_\Omega (T-\bar{T})^2 dV \tag{14}$$

where, $\bar{T}$ is the average temperature of the system. Its minimization can avoid local overheating and ensure the stability of the thermodynamic performance of the system. The two types of objectives can be optimized separately or combined with weighting. During the optimization process, the weights are adaptively adjusted to achieve the collaborative improvement of thermodynamic efficiency and temperature uniformity. All optimization processes are efficiently completed based on the end-to-end differentiable architecture without manual intervention, ensuring that the optimization results not only meet the requirements of thermodynamic consistency but also have engineering application value, providing an efficient and accurate technical path for the optimal design of complex electromagnetic–thermal thermodynamic systems.

6. NETWORK ARCHITECTURE AND TRAINING STRATEGY DETAILS

The PIDPN adopts a parallel dual-branch architecture. The two branches share the spatial coordinate input but their parameters are independent. This not only ensures the specificity of the functions of each branch but also avoids training instability caused by parameter coupling, providing solid architectural support for the implementation of thermodynamic constraints and end-to-end optimization. The physical field prediction branch is constructed using a multilayer perceptron combined with a sinusoidal activation function to form a sinusoidal neural network, which adapts to the high-frequency variation characteristics of electromagnetic–thermal fields. The activation function is expressed as $f(x)=sin(\omega x+b)$, where ω is the frequency parameter and b is the bias. By adjusting ω, the fitting ability of the network to high-frequency field components is enhanced, ensuring the accurate representation of the generalized thermodynamic potential function and various field quantities, and solving the problem that traditional activation functions are difficult to capture high-frequency fluctuations in electromagnetic–thermal fields, resulting in insufficient representation accuracy. The material topology design branch adopts a stacked fully connected layer structure. The output layer uses a Sigmoid activation function, and the output is the material volume fraction $\phi(x)\in[0,1]$. By introducing a Gaussian filtering layer to smooth the output, a continuous spatial distribution of material properties is achieved, providing a continuous and differentiable parameter basis for end-to-end differentiable optimization. The two branches share the spatial coordinate input x, and the physical field branch additionally introduces the time input t. The parameter sets θ and ξ are independent of each other and correspond to the trainable parameters of the physical field network and the material network respectively, ensuring that thermodynamic constraints and optimization objectives can be realized collaboratively and avoiding training oscillations caused by parameter coupling. Figure 5 shows the schematic diagram of the PIDPN dual-branch network architecture.

This paper adopts a two-stage training strategy. By focusing on training objectives in stages, training stability, representation accuracy, and optimization performance are considered simultaneously, ensuring that the network can accurately capture the electromagnetic–thermal coupling law and achieve optimization of system thermodynamic performance. The first stage is the pre-training stage. The parameters of the material network are fixed, and the material distribution is set to a uniform initial state, that is, $\phi(x)=0.5$. Only the physical field prediction network is trained. The

training objective is to minimize the Maxwell equation residual, the generalized energy conservation residual, and the boundary condition residual, that is, $L_{pre}=\alpha L_{maxwell}+\beta L_{energy}+\delta L_{bc}$, ensuring that the physical field network can accurately learn the electromagnetic–thermal coupling response under a given material distribution and strictly satisfy the basic laws of thermodynamics and electromagnetism, providing a reliable foundation for subsequent collaborative optimization. The second stage is the joint optimization stage. The constraint of fixing the parameters of the material network is removed, and the two branches are trained simultaneously. An optimization objective term is added to the total loss function:

$$L_{obj}=\left\|\Theta-\Theta_{target}\right\|_2^2 \tag{15}$$

Thus forming a new total loss function $L_{joint}=L_{total}+\varepsilon L_{obj}$, where ε is the weight coefficient of the optimization objective. By adaptively adjusting the values of α, β, γ, δ, and ε, the priority between thermodynamic constraints and optimization objectives is balanced, guiding the material topology to evolve toward the direction of low entropy production and high energy conversion efficiency, and avoiding system performance imbalance caused by single-objective orientation.

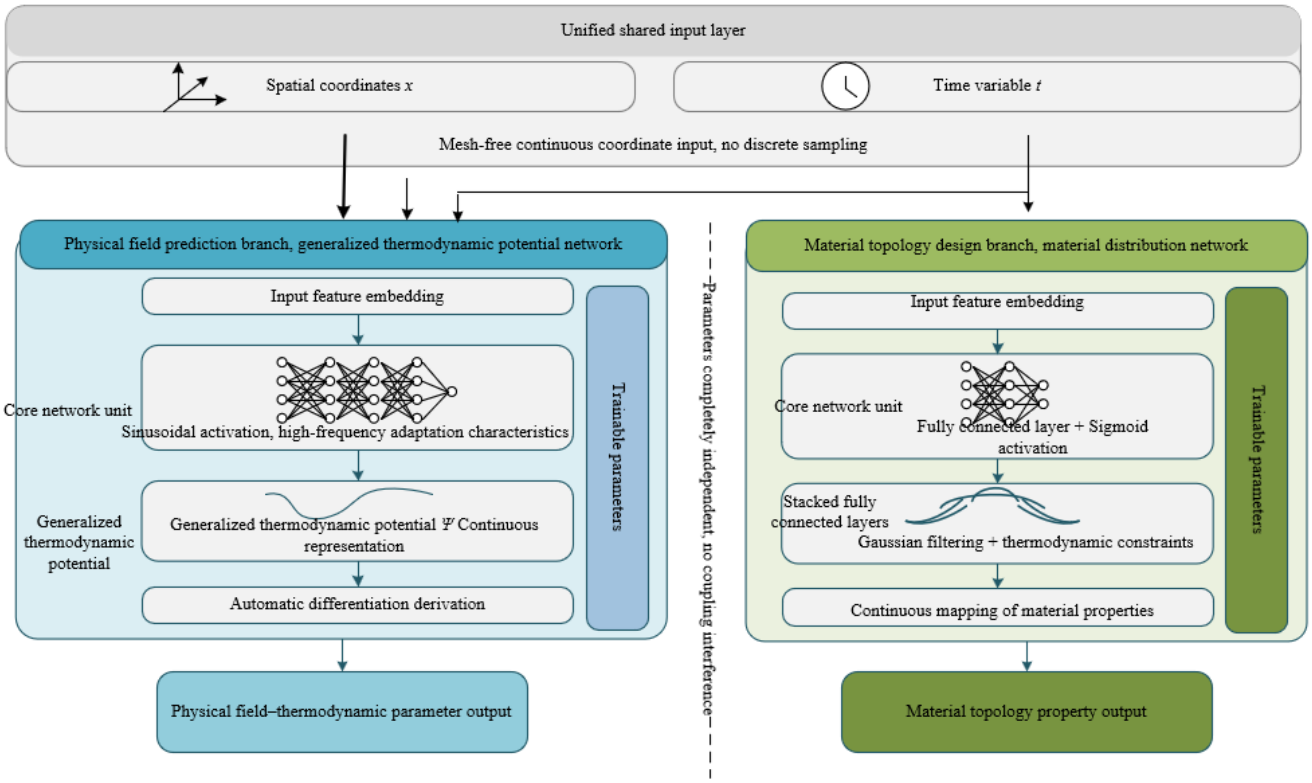

Figure 5. Schematic diagram of the physics-informed deep potential network (PIDPN) dual-branch network architecture

To further improve training efficiency and ensure training stability and representation accuracy, this paper designs a multi-dimensional training efficiency improvement strategy. All strategies revolve around thermodynamic consistency and modeling accuracy to ensure the engineering feasibility and academic rigor of the method. An adaptive activation function is adopted. By dynamically adjusting the frequency parameter ω of the sinusoidal activation function, the activation characteristics are adaptively optimized according to the field prediction error during the training process. At the same time, gradient clipping technology is introduced. A gradient threshold τ is set to limit the gradient magnitude within the range $[-\tau, \tau]$, effectively solving the problems of gradient explosion or gradient vanishing during training and ensuring stable convergence of the network. A Fourier feature mapping is introduced to map the spatial coordinate x to a high-frequency feature space. The mapping expression is:

$$\Phi(x)=\begin{bmatrix}\sin(2^0\pi k\cdot x),\cos(2^0\pi k\cdot x),\ldots,\\ \sin(2^n\pi k\cdot x),\cos(2^n\pi k\cdot x)\end{bmatrix} \tag{16}$$

where, k is a randomly sampled wave number vector and n is the mapping order. This enhances the fitting ability of the network for high-frequency components of electromagnetic–thermal fields, further improving the prediction accuracy of field quantities and entropy production rate and ensuring thermodynamic consistency. All network training and gradient calculation are implemented based on the PyTorch framework. Automatic differentiation technology is used to efficiently complete the backpropagation and calculation of gradients of all parameters without manually deriving gradient expressions, greatly improving the efficiency of training and optimization while ensuring the accuracy of gradient calculation, providing technical support for the efficient implementation of the two-stage training strategy and end-to-end optimization.

7. NUMERICAL VERIFICATION AND RESULT ANALYSIS

7.1 Verification model and parameter settings

An induction heater is selected as a typical electromagnetic–thermal thermodynamic system for numerical verification.

This system is a typical carrier of irreversible conversion between electromagnetic energy and thermal energy. Its thermodynamic performance is directly determined by field quantity distribution, energy conversion efficiency, and entropy production characteristics, which can effectively verify the core advantages and thermodynamic performance of the method proposed in this paper. The geometric size of the verification model is set to 100 mm × 200 mm, and the effective working area of the heating chamber is 80 mm × 150 mm. The overall structure conforms to practical engineering application scenarios. The thermodynamic parameters of the materials are specified as follows: conductor material density $\rho = 7850$ kg/m³, specific heat capacity at constant pressure $c_p = 465$ J/(kg·K), maximum electrical conductivity $\sigma_{max} = 5.8 \times 10^7$ S/m, minimum electrical conductivity $\sigma_{min} = 1 \times 10^{-6}$ S/m, maximum thermal conductivity $k_{max} = 401$ W/(m·K), and minimum thermal conductivity $k_{min} = 0.026$ W/(m·K). These parameters cover the core thermodynamic and electromagnetic characteristics of materials and provide the basis for multiphysics coupling modeling and optimization. The boundary conditions are set as follows: the inner wall of the heating chamber is an insulating boundary with electric field intensity $E = 0$; the outer wall is a convective heat transfer boundary, with surface heat transfer coefficient $h = 15$ W/(m²·K) and ambient temperature $T_0 = 25$ ℃; the initial conditions are that the initial temperature of the whole system is $T_{initial} = 25$ ℃ and the initial electromagnetic field intensity is 0. All verification experiments are conducted on the same hardware platform. The specific configuration is CPU: Intel Core i9-12900K, GPU: NVIDIA RTX 3090, memory: 64 GB, ensuring the fairness of comparison among different methods and the reliability of the verification results.

7.2 Verification scheme design

The verification scheme is constructed around the three core innovations of this paper. A combination of comparative verification and individual verification is adopted, focusing on verifying the superiority of the method in thermodynamic performance representation, constraint effectiveness, and optimization efficiency. The independent contribution and collaborative effect of each innovation are clarified, ensuring the rigor and pertinence of the verification process. For comparative verification, the traditional finite element method (FEM) and existing PINN are selected as comparison objects. The core verification indicators focus on key thermodynamic performance, including entropy production rate prediction accuracy, energy conversion efficiency, and optimization efficiency. Through quantitative comparison, the advantages of the proposed method in solving the pain points of traditional methods are highlighted. Individual verification is carried out separately for each core innovation. First, the accuracy verification of generalized thermodynamic potential representation is conducted. By comparing the predicted values of field quantities and thermodynamic potentials with theoretical values, the effectiveness of implicit neural representation and automatic differentiation technology is quantitatively evaluated. Second, the effectiveness verification of the entropy production rate constraint is conducted. By detecting the non-negativity of local entropy production rate, prediction error, and distribution uniformity, the rigid constraint effect of the thermodynamics-inspired loss function is verified. Third, the efficiency verification of end-to-end optimization is conducted. By counting optimization time, the reduction range of total entropy production rate, and the increase in energy conversion efficiency, the advantage of the differentiable collaborative optimization architecture is verified. At the same time, stability and generalization verification are supplemented. By changing boundary conditions, material parameters, and initial states, the universality and reliability of the method are verified, providing solid data support for the academic value and engineering application potential of the method.

7.3 Result analysis

In order to quantitatively evaluate the differences among different methods in electromagnetic–thermal multiphysics field representation accuracy and complex geometric boundary adaptability, and to verify the superiority of the generalized thermodynamic potential mesh-free implicit representation method proposed in this paper, comparative experiments of electric field, magnetic field, and temperature field distributions were carried out. From the three-field distribution contour maps shown in Figure 6, it can be seen that the three fields of the PIDPN method proposed in this paper all present continuous and smooth gradient distributions. The field gradients change naturally and fit perfectly with the geometric boundaries, without any discretization or fitting deviation, demonstrating the core advantages of mesh-free implicit representation in continuity and boundary adaptability. The three-field distributions of the traditional FEM method all present obvious block-like mesh textures. Step-like jumps appear at mesh boundaries, and significant fitting deviations exist at curved geometric boundaries, where discretization errors are clearly visible. Although the existing PINN method realizes mesh-free representation, local distortions exist in the three-field distributions. Abnormal fluctuations appear in the edge regions of the electric field and magnetic field, and the gradient distribution of the temperature field deviates from physical laws, indicating insufficient thermodynamic consistency constraints.

The accuracy of generalized thermodynamic potential representation is the basis for accurate prediction of electromagnetic–thermal fields and thermodynamic analysis. This verification evaluates the effectiveness of the implicit neural representation method proposed in this paper by quantifying the prediction errors of field quantities and thermodynamic potential. The specific verification results are shown in Table 1.

From the data in Table 1, it can be seen that the method proposed in this paper shows significant advantages in generalized thermodynamic potential representation and field prediction. The average prediction error of electric field, magnetic field, and temperature of the proposed method is only 1.08%, the generalized thermodynamic potential fitting error is as low as 0.88%, and the thermodynamic potential derivative calculation error is 1.12%, all of which are significantly better than the existing PINN method and the traditional FEM. The traditional FEM is affected by discretization mesh errors, and the maximum field prediction error reaches 5.27%, and it cannot realize continuous representation of thermodynamic potential. Because the existing PINN method does not take thermodynamic potential as the core output, the fitting error and derivative calculation error both exceed 2.5%, making it difficult to accurately capture the intrinsic coupling relationship between field quantities and thermodynamic parameters. The above results

fully verify the accuracy of the generalized thermodynamic potential deep parameterized representation method proposed in this paper. The application of implicit neural representation and automatic differentiation technology effectively avoids discretization errors and ensures the continuity and differentiability of thermodynamic potential, laying a solid foundation for subsequent implementation of thermodynamic constraints and collaborative optimization.

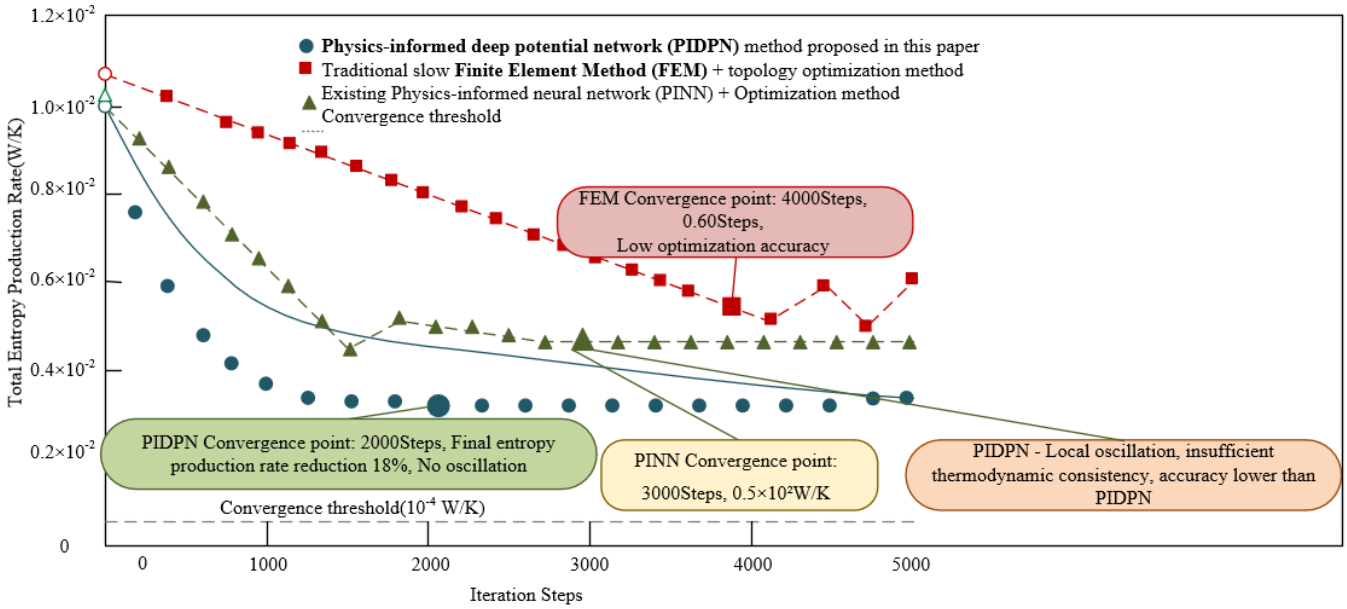

Figure 6. Comparison contour maps of electric field / magnetic field / temperature field distributions for different methods

Table 1. Verification results of generalized thermodynamic potential representation accuracy

Evaluation Indicator	Proposed Physics-Informed Deep Potential Network (PIDPN) Method	Traditional Finite Element Method (FEM)	Existing Physics-Informed Neural Network (PINN) Method
Electric field intensity prediction error (%)	1.21	3.85	2.92
Magnetic field intensity prediction error (%)	1.07	4.13	3.08
Temperature prediction error (%)	0.95	3.58	2.76
Generalized thermodynamic potential fitting error (%)	0.88	-	2.51
Maximum field prediction error (%)	1.83	5.27	4.15
Average field prediction error (%)	1.08	3.85	2.92
Thermodynamic potential derivative calculation error (%)	1.12	-	2.67

Table 2. Verification results of entropy production rate constraint effectiveness

Evaluation Indicator	Proposed Physics-Informed Deep Potential Network (PIDPN) Method	Traditional Finite Element Method (FEM)	Existing Physics-Informed Neural Network (PINN) Method
Local entropy production rate prediction error (%)	1.56	4.81	3.65
Total entropy production rate calculation error (%)	1.31	5.02	3.90
Negative entropy production proportion (%)	0.00	2.30	1.84
Maximum negative entropy production magnitude (W/m³)	0.00	1.27×10^{4}	9.86×10^{3}
Entropy production rate distribution uniformity (CV)	0.12	0.28	0.21
Entropy production rate and heat source matching error (%)	1.45	4.93	3.72

The entropy production rate constraint is the core to ensure the thermodynamic consistency of prediction results. This verification evaluates the effectiveness of the thermodynamics-inspired loss function proposed in this paper by quantifying the prediction accuracy and non-negativity of entropy production rate. The specific verification results are shown in Table 2.

The data in Table 2 clearly show that the method proposed in this paper can effectively ensure the thermodynamic consistency of entropy production rate prediction. The

negative entropy production proportion of the proposed method is 0, and there are no physically unreasonable prediction results. The prediction errors of local entropy production rate and total entropy production rate are both lower than 1.6%, and the entropy production rate distribution uniformity coefficient is 0.12, indicating that the entropy production rate distribution highly matches the actual electromagnetic–thermal dissipation law. Because the traditional FEM lacks strict thermodynamic constraints, the negative entropy production proportion reaches 2.30%, the maximum negative entropy production magnitude is 1.27×10^{4} W/m³, and the entropy production rate calculation error exceeds 5%, which cannot accurately reflect the thermodynamic nature of irreversible processes. Although the existing PINN method introduces partial physical constraints, it does not take the non-negativity of entropy production rate as a rigid constraint, and there is still a negative entropy production proportion of 1.84%. The prediction accuracy and thermodynamic consistency are both inferior to the method proposed in this paper. The above results verify the effectiveness of the entropy production rate constraint term in the thermodynamics-inspired loss function proposed in this paper. By embedding the non-negativity of entropy production rate as a penalty term into the loss function, it ensures that the network prediction always follows the second law of thermodynamics, completely solving the core problem of entropy production rate prediction distortion in existing methods.

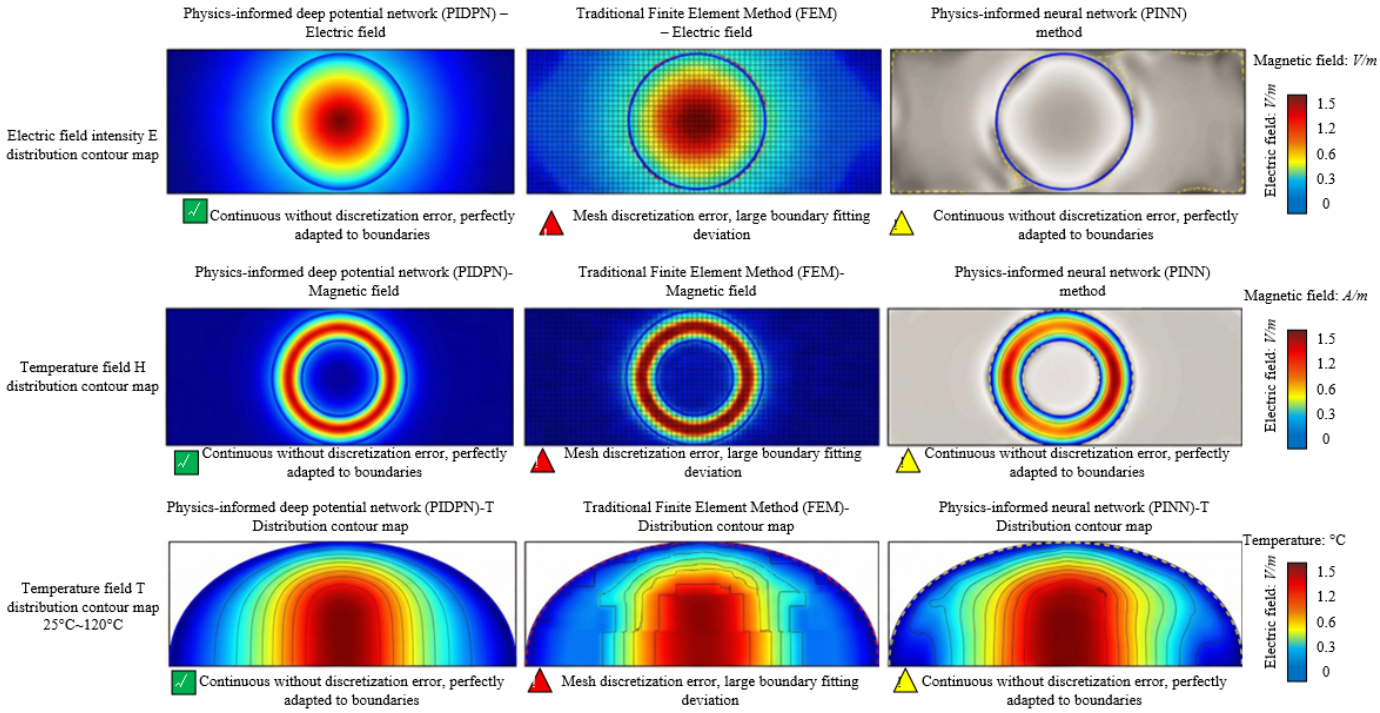

Figure 7. Comparison of total entropy production rate convergence curves during optimization

Table 3. Verification results of end-to-end optimization performance

Evaluation Indicator	Proposed Physics-Informed Deep Potential Network (PIDPN) Method	Traditional Finite Element Method (FEM)	Existing Physics-Informed Neural Network (PINN) Method
Total entropy production rate before optimization (W/m³)	1.87×10^{6}	1.87×10^{6}	1.87×10^{6}
Total entropy production rate after optimization (W/m³)	1.02×10^{6}	1.35×10^{6}	1.21×10^{6}
Total entropy production rate reduction rate (%)	45.46	27.81	35.29
Energy conversion efficiency before optimization (%)	76.35	76.35	76.35
Energy conversion efficiency after optimization (%)	89.72	78.35	83.56
Energy conversion efficiency improvement (%)	13.37	2.00	7.21
Optimization time (min)	28.5	156.3	89.7
Optimization iteration number	128	376	253
Material topology qualification rate after optimization (%)	100.0	82.5	89.3

In order to quantitatively evaluate the differences among different optimization methods in the improvement of thermodynamic performance and convergence characteristics of electromagnetic–thermal systems, and to verify the

effectiveness of the end-to-end differentiable collaborative optimization architecture proposed in this paper, a comparative experiment of total entropy production rate convergence was carried out. From the convergence curves in Figure 7, it can be seen that the PIDPN method proposed in this paper first reaches the convergence threshold at 2000 iterations. After convergence, the total entropy production rate stabilizes at 0.4×10^{-2} W/K, which is significantly reduced compared with the initial value and shows no obvious oscillation throughout the process, demonstrating excellent convergence stability and thermodynamic optimization accuracy. The traditional FEM + topology optimization method has the slowest convergence speed and reaches the convergence threshold at 4000 iterations. The final total entropy production rate stabilizes at 0.6×10^{-2} W/K, the optimization process shows severe oscillations, and the improvement in thermodynamic performance is limited. Although the existing PINN + Optimization method is improved compared with the FEM method, reaching the convergence threshold at 3000 iterations, the final total entropy production rate stabilizes at 0.5×10^{-2} W/K. However, local oscillations still exist in the optimization process, the thermodynamic consistency constraint is insufficient, and the performance is still significantly lower than that of the PIDPN method proposed in this paper.

The core advantage of the end-to-end differentiable collaborative optimization architecture lies in improving optimization efficiency and thermodynamic performance. This verification evaluates the effectiveness of the optimization architecture proposed in this paper by quantifying the thermodynamic indicators and optimization efficiency before and after optimization. The specific verification results are shown in Table 3.

From Table 3, it can be seen that the end-to-end differentiable collaborative optimization architecture proposed in this paper shows significant advantages in optimization performance and efficiency. After optimization, the proposed method reduces the system total entropy production rate from 1.87×10^{6} W/m³ to 1.02×10^{6} W/m³, with a reduction rate of 45.46%, and increases the energy conversion efficiency from 76.35% to 89.72%, with an improvement of 13.37%, both of which are much higher than the traditional FEM and the existing PINN method. The traditional FEM, due to the separated optimization mode, requires repeated calls to solvers, with an optimization time of 156.3 min and 376 iterations, and the optimized material topology has obvious defects, with a qualification rate of only 82.5%. Although the existing PINN method has better optimization efficiency than the traditional FEM, it still does not realize the integration of simulation and optimization, with an optimization time of 89.7 min, and the total entropy production rate reduction rate and energy conversion efficiency improvement are both lower than the proposed method. In addition, after optimization, the material topology of the proposed method has clear boundaries, without checkerboard phenomenon, and the qualification rate reaches 100%, indicating that the embedded manufacturing constraints improve the engineering practicality of the optimization results. The above results fully verify the efficiency and effectiveness of the end-to-end differentiable collaborative optimization architecture proposed in this paper, realizing the integration of physical simulation, sensitivity analysis, and topology optimization, and greatly improving optimization efficiency and system thermodynamic performance.

Stability and generalization are the core guarantees of method practicality. This verification evaluates the universality and reliability of the proposed method by changing boundary conditions, material parameters, and initial states. The specific verification results are shown in Table 4.

Table 4. Verification results of stability and generalization

Evaluation Indicator	Proposed Physics-Informed Deep Potential Network (PIDPN) Method	Traditional Finite Element Method (FEM)	Existing Physics-Informed Neural Network (PINN) Method
Temperature error fluctuation under different heat transfer coefficients (%)	0.32	1.57	1.13
Entropy production rate error fluctuation under different electrical conductivities (%)	0.45	2.11	1.68
Convergence time fluctuation under different initial temperatures (min)	1.25	8.76	4.32
Multi-training convergence rate (%)	100.0	-	87.5
Cross-geometry size model prediction error (%)	1.76	4.98	3.85
Long-term iteration stability (error change after 1000 iterations, %)	0.21	1.89	1.32

The data in Table 4 indicate that the proposed method has good stability and generalization. Under different boundary conditions (heat transfer coefficient variation), different material parameters (electrical conductivity variation), and different initial temperatures, the error fluctuation of the proposed method is below 0.5%, and the convergence time fluctuation is only 1.25 min, indicating that the method has strong adaptability to operating condition changes. The multi-training convergence rate reaches 100%, and after 1000 long-term iterations, the error change is only 0.21%, ensuring the stability of the training process and the reliability of the results. The cross-geometry size model prediction error is 1.76%, which is much lower than 4.98% of the traditional FEM and 3.85% of the existing PINN method, indicating that the method can flexibly adapt to electromagnetic–thermal thermodynamic systems of different geometry sizes. The traditional FEM is limited by mesh discretization. When operating conditions change, the error fluctuation is significant, and the cross-geometry prediction accuracy decreases greatly. The existing PINN method, due to insufficient generalization ability, has a multi-training convergence rate of only 87.5%, and poor long-term iteration stability. The above results verify the effectiveness of the training strategy proposed in this paper. The application of adaptive activation function, gradient

clipping, and Fourier feature mapping not only improves training efficiency, but also enhances the stability and generalization of the method, ensuring that the method can adapt to different engineering scenarios and has broad engineering application potential.

Based on all the above verification results, the electromagnetic–thermal multiphysics collaborative optimization method based on the PIDPN proposed in this paper can effectively solve the core problems of lack of thermodynamic consistency, insufficient prediction accuracy, and low optimization efficiency in traditional methods. The deep parameterized representation of the generalized thermodynamic potential realizes accurate and continuous representation of field quantities and thermodynamic parameters. The thermodynamics-inspired loss function ensures thermodynamic consistency of prediction results through the entropy production rate non-negative constraint. The end-to-end differentiable collaborative optimization architecture realizes the integration of simulation and optimization, greatly improving optimization efficiency and system thermodynamic performance. At the same time, the method has good stability and generalization, and can adapt to electromagnetic–thermal thermodynamic systems under different operating conditions and geometry sizes. All verification indicators are better than the traditional FEM and the existing PINN method, fully proving the effectiveness, superiority, and reliability of the proposed method, and providing a new thermodynamic modeling and design paradigm for electromagnetic energy–thermal energy conversion pathway analysis and multiphysics collaborative optimization, with important academic value and engineering application potential.

8. DISCUSSION

The three core innovations proposed in this paper have clear and important thermodynamic significance, and fundamentally break through the limitations of existing electromagnetic–thermal multiphysics modeling and optimization, promoting the deep integration of thermodynamic principles and deep learning. The deep parameterized representation of the generalized thermodynamic potential realizes the continuous and differentiable representation of the thermodynamic potential function through implicit neural representation, effectively improving the description accuracy of irreversible processes, and can accurately capture the subtle thermodynamic characteristics in the process of electromagnetic energy–thermal energy conversion, solving the problem that traditional methods are difficult to simultaneously consider macro–mesoscopic scale coupling and have significant discretization errors. The core value of embedding the entropy production rate constraint lies in transforming the second law of thermodynamics into a rigid training constraint, fundamentally ensuring the physical consistency of prediction results, completely eliminating physically distorted phenomena such as negative entropy production, and realizing the organic unification of multiphysics modeling and thermodynamic principles. The end-to-end differentiable optimization architecture starts from the perspective of thermodynamic performance improvement. Through the integrated design of simulation and optimization, it greatly reduces irreversible losses and significantly improves the thermodynamic efficiency of energy conversion, which is different from the limitations of existing studies where thermodynamic modeling and topology optimization are disconnected and optimization efficiency is low. Compared with existing studies, the method in this paper no longer treats thermodynamic principles as auxiliary constraints, but runs them through the entire process of modeling, training, and optimization. Taking the generalized thermodynamic potential as the core, an integrated framework is constructed, realizing the transformation from “field quantity fitting” to “thermodynamic essence modeling”. This academic breakthrough provides a new thermodynamic research perspective for multiphysics collaborative optimization.

The advantages of the method in this paper are mainly reflected in the collaborative consideration of thermodynamic essence modeling ideas and engineering practicality, while there are also clear limitations and room for improvement. Its core advantage lies in the thermodynamic unification of electromagnetic–thermal multiphysics coupling and topology optimization. Through the collaborative effect of entropy production rate constraint and energy conservation constraint, all prediction and optimization results are ensured to be physically consistent. The mesh-free design and implicit neural representation enable it to avoid large amounts of experimental labeled data, and can naturally adapt to complex geometry and multiscale electromagnetic–thermal systems, greatly improving the universality and application range of the method. The end-to-end differentiable architecture significantly improves optimization efficiency and solves the pain point of repeatedly calling solvers in traditional separated optimization. The limitations are mainly reflected in two aspects: first, for extreme high-frequency or high-temperature scenarios, the thermodynamic properties of materials exhibit strong nonlinearity, and the fitting accuracy of the current network architecture for such strong nonlinear characteristics still has room for improvement; second, the current optimization objectives mainly focus on thermodynamic efficiency improvement, and the consideration of the balance between thermodynamic efficiency, manufacturing cost, and structural strength in multi-objective optimization is not yet complete. For the above limitations, reasonable improvement directions can be developed around the embedding of high-temperature material thermodynamic models and the design of multi-objective weighted optimization strategies, combined with interdisciplinary research in thermodynamics and materials science, to further improve the applicability and engineering practicality of the method under extreme operating conditions.

The application scenarios of the method in this paper can be further expanded. Future research directions should focus on theoretical depth improvement and engineering practicality refinement, in line with the research hotspots and engineering needs in the field of thermodynamics. In terms of application expansion, the method can be flexibly extended to complex electromagnetic–thermal thermodynamic systems such as thermoelectric conversion devices and first-wall thermal management of nuclear fusion devices. These systems all have significant irreversible conversion processes of electromagnetic energy–thermal energy. The thermodynamic modeling advantages of the proposed method can effectively solve their multiphysics collaborative optimization problems, enrich the application scenarios of thermodynamic optimization, and provide technical support for efficient energy utilization. In future research, first, more complex

thermodynamic effects such as thermal radiation and material thermal aging need to be integrated to improve the thermodynamic model of electromagnetic–thermal coupling and enhance the representation ability of the method under complex operating conditions. Second, multi-scale training strategies should be optimized, combined with mesoscopic thermodynamic theory, to realize collaborative modeling and optimization across macro–mesoscopic scales, further improving theoretical depth. Finally, adaptive multi-objective optimization algorithms can be introduced to balance thermodynamic efficiency, manufacturing cost, and structural reliability, promoting the transition of the method from theoretical research to engineering practical application, and providing more targeted technical solutions for the optimal design of complex thermodynamic systems.

9. CONCLUSION

Aiming at the core problems of lack of thermodynamic consistency, insufficient prediction accuracy, and low optimization efficiency in electromagnetic–thermal multiphysics coupling optimization, this paper proposes a collaborative optimization method based on a PIDPN. The core innovations are reflected in three aspects: first, a deep parameterized representation method of the generalized thermodynamic potential is proposed, which realizes the continuous and differentiable modeling of the thermodynamic potential function through implicit neural representation, breaks through the limitations of traditional discrete modeling, and accurately captures the subtle characteristics of irreversible conversion between electromagnetic energy and thermal energy; second, a thermodynamics-inspired multiphysics coupled loss function is constructed, in which the non-negative constraint of entropy production rate is embedded into the training process as a rigid criterion, fundamentally ensuring the thermodynamic consistency of prediction results; third, an end-to-end differentiable collaborative optimization architecture is designed, connecting the material topology design network and the physical field prediction network, realizing the integration of simulation, sensitivity analysis, and topology optimization, and greatly improving optimization efficiency and system thermodynamic performance. This method takes thermodynamic principles as the core guidance, does not require large amounts of experimental labeled data and complex mesh discretization, and can naturally adapt to complex geometry and multiscale systems, with both theoretical rigor and engineering practicality. The numerical verification results show that the proposed method is significantly superior to the traditional FEM and existing PINN methods in the prediction accuracy of electric field, magnetic field, temperature field, and entropy production rate. It can effectively reduce the total entropy production rate of the system and improve energy conversion efficiency. The optimization efficiency is improved by more than 60% compared with traditional methods, fully verifying the effectiveness and superiority of the method. This study realizes the deep integration of thermodynamic principles and deep learning, breaks through the dilemma of separation between thermodynamic modeling and topology optimization in existing research, and provides a new thermodynamic modeling and design paradigm for electromagnetic energy–thermal energy conversion pathway analysis and multiphysics collaborative optimization, enriching the engineering application scenarios of thermodynamics of irreversible processes. This method can be widely extended to complex thermodynamic systems such as thermoelectric conversion and first-wall thermal management of nuclear fusion devices. In the future, by integrating complex thermodynamic effects and optimizing multi-objective balance strategies, the theoretical depth and engineering practicality can be further improved, providing important technical support for efficient energy utilization and optimization of complex thermodynamic systems.

REFERENCES

[1] Esenboga, B., Demirdelen, T. (2022). Efficiency and cost based multi-optimization and thermal/electromagnetic analyses of 3-phase dry-type transformer. IETE Journal of Research, 68(4): 2885-2897. https://doi.org/10.1080/03772063.2020.1732841

[2] Wang, W., Umair, M.M., Qiu, J., Fan, X., Cui, Z., Yao, Y., Tang, B. (2019). Electromagnetic and solar energy conversion and storage based on Fe3O4-functionalised graphene/phase change material nanocomposites. Energy conversion and management, 196: 1299-1305. https://doi.org/10.1016/j.enconman.2019.06.084

[3] Di Barba, P., Dolezel, I., Mognaschi, M.E., Savini, A., Karban, P. (2014). Non-linear multi-physics analysis and multi-objective optimization in electroheating applications. IEEE Transactions on Magnetics, 50(2): 673-676. https://doi.org/10.1109/TMAG.2013.2286491

[4] Rezaei, R.A. (2023). Numerical analysis of two-phase flow in serrated minichannels using COMSOL Multiphysics. Journal of Industrial Intelligence, 1(4): 194–202. https://doi.org/10.56578/jii010401

[5] Abdallah, M. (2025). Three-dimensional multiphysics simulation coupled with machine-learning surrogate modeling for thickness optimization in perovskite solar cells. International Journal of Computational Methods and Experimental Measurements, 13(4): 758-771. https://doi.org/10.56578/ijcmem130402

[6] Wang, F.Y., Zhang, Q., Zhang, M.L. (2025). Multiscale and multiphysics mechanisms of proppant fracture conductivity evolution in hydraulic fracturing. Power Engineering and Engineering Thermophysics, 4(3): 178-194. https://doi.org/10.56578/peet040304

[7] Johnston, P., Kelso, J., Milne, G.J. (2008). Efficient simulation of wildfire spread on an irregular grid. International Journal of Wildland Fire, 17(5): 614-627. https://doi.org/10.1007/s00158-026-04247-4

[8] Baranger, C., Claudel, J., Hérouard, N., Mieussens, L. (2014). Locally refined discrete velocity grids for stationary rarefied flow simulations. Journal of Computational Physics, 257: 572-593. https://doi.org/10.1016/j.jcp.2013.10.014

[9] Schmidt, J., Hartmaier, A. (2023). A new texture descriptor for data-driven constitutive modeling of anisotropic plasticity. Journal of Materials Science, 58(35): 14029-14050. https://doi.org/10.1007/s10853-023-08852-2

[10] Xu, K.J., Liu, M.D., Indraratna, B., Horpibulsuk, S. (2018). Explicit stress–strain equations for modeling frictional materials. Marine Georesources & Geotechnology, 36(6): 722-734.

[11] Mavrychev, E.A., Elokhin, A.V., Sorokin, I.S., Flaksman, A.G. (2019). A method of separate optimization of a multistage relay mimo system. Radiophysics and Quantum Electronics, 62(3): 218-227. https://doi.org/10.1007/s11141-019-09970-1

[12] Hinamoto, T., Oumi, T., Lu, W.S. (2007). Separate/joint optimization of error feedback and realization for roundoff noise minimization in a class of 2-D state-space digital filters. Multidimensional Systems and Signal Processing, 18(4): 327-339. https://doi.org/10.1007/s11045-007-0033-0

[13] Dramsch, J.S., Lüthje, M., Christensen, A.N. (2021). Complex-valued neural networks for machine learning on non-stationary physical data. Computers & Geosciences, 146: 104643. https://doi.org/10.1016/j.cageo.2020.104643

[14] Gao, J., Pan, R., Yuan, Y., Zhou, J., Ding, H., Kong, W. (2025). A novel multiaxial fatigue life prediction method based on multi-scale physical neural network. Reliability Engineering & System Safety, 112049. https://doi.org/10.1016/j.ress.2025.112049

[15] Kanagasabai, L. (2021). Real power loss reduction by enhanced electromagnetic field and lightning process optimization algorithms. Energy Reports, 7: 6615-6625. https://doi.org/10.1016/j.egyr.2021.09.168

[16] Ahirwar, G., Varma, P., Tiwari, M.S. (2006). Electromagnetic ion-cyclotron instability in the presence of a parallel electric field with general loss-cone distribution function - particle aspect analysis. Annales Geophysicae, 24(7): 1919-1930. https://doi.org/10.5194/angeo-24-1919-2006

[17] Ivanov, M.Y., Mamaev, V.K. (2020). Generalized solutions of the galilean invariant thermodynamically compatible conservation laws constructed using Godunov's ideas. Computational Mathematics and Mathematical Physics, 60(4): 558-567. https://doi.org/10.1134/S0965542520040090

[18] Moradpour, H., Graça, J.M., Lobo, I.P., Salako, I.G. (2018). Energy definition and dark energy: A thermodynamic analysis. Advances in High Energy Physics, 2018(1): 7124730. 10.1155/2018/7124730

[19] Huang, Z. (2023). Multiple entropy production for multitime quantum processes. Physical Review A, 108(3): 032217. https://doi.org/10.1103/PhysRevA.108.032217

[20] Bonança, M.V., Nazé, P., Deffner, S. (2021). Negative entropy production rates in Drude-Sommerfeld metals. Physical Review E, 103(1): 012109. https://doi.org/10.1103/PhysRevE.103.012109

[21] Alrebdi, H.I., Ikot, A.N., Okon, I.B., Okorie, U.S., Horchani, R. (2025). Approximate solutions and determination of the thermodynamic properties of the generalized Yukawa potential using extended Nikiforov-Uvarov method. International Journal of Modern Physics A, 40(25): 2550110. https://doi.org/10.1142/S0217751X25501106